SECED 2015 Conference: Earthquake Risk and Engineering towards a Resilient World
9-10 July 2015, Cambridge UK

COMPARISON OF SEISMIC ECONOMIC LOSSES IN MULTI-STOREY STEEL BUILDINGS WITH VISCOUS DAMPERS AND CONVENTIONAL OR SELF-CENTERING STEEL MRFs

Athanasios I. Dimopoulos [1], Angelos S. Tzimas[2], Dimitrios Vamvatsikos [3] and Theodore L. Karavasilis [4]

Abstract: This paper evaluates the potential of self-centering moment-resisting frames (SC-MRFs) with viscous dampers to reduce the economic losses in steel buildings due to strong earthquakes. The evaluation is based on the comparison of different designs of a prototype steel building using as lateral-load resisting system: 1) conventional steel moment resisting frames (MRFs); 2) MRFs and viscous dampers; 3) SC-MRFs; and 4) SC-MRFs with viscous dampers. The economic losses are estimated by developing vulnerability functions according to the ATC-58 methodology. The influence of residual storey drifts on economic losses is examined by accounting for the possibility of having to demolish a building as a result of excessive residual storey drifts. Results highlight the importance of considering residual story drifts as a demand parameter to economic loss estimation; and show that the use of viscous dampers significantly improves the building's performance for both SC-MRF and MRF, resulting in lower repair cost.

Introduction

Conventional seismic resistant structures are designed to sustain significant inelastic deformations in main structural members under the design basis earthquake (DBE) (EC8 2008). Inelastic deformations result in damage and residual drifts, and so, in economic losses such as repair costs and downtime. Steel self-centering moment-resisting frames (SC-MRFs) using post-tensioned (PT) beam-column connections are a promising class of resilient structures. SC-MRFs exhibit softening force-drift behaviour and eliminate beam inelastic deformations and residual drifts as the result of gap openings developed in beam-column interfaces and elastic PT bars which clamp beams to columns and provide self-centering capability. PT connections use energy dissipation devices which are activated when gaps open and can be easily replaced if damaged. However, existing design procedures (Garlock et al. 2007; Kim and Christopoulos 2008) aim to achieve peak drifts similar to those of conventional steel moment resisting frames (MRFs), and so, accept appreciable damage in drift-sensitive non-structural elements. To address this issue, a seismic design strategy developed by Tzimas et al. (2015) use viscous dampers in parallel to SC-MRFs, to effective control the structural and non-structural damage by simultaneously controlling beam plastic deformations, peak storey drifts, and residual storey drifts.

To the authors knowledge the potential of SC-MRFs and SC-MRFs with viscous dampers to reduce economic seismic losses by simultaneously controlling structural and non-structural damage has not been quantified yet. Such quantification is of particular interest to justify the increased cost and design complexity of SC-MRFs with and without viscous dampers in comparison to MRFs with and without viscous dampers.

[1] *PhD student, School of Engineering, University of Warwick, Coventry, UK*
E-mail: A.Dimopoulos@warwick.ac.uk
[2] *Post-Doctoral Research Fellow, School of Engineering, University of Warwick, Coventry, UK*
A.Tzimas@warwick.ac.uk
[3] *Lecturer, School of Engineering, NTU, Athens, Greece*
Dvamva@mail.ntua.gr
[4] *Associate Professor, School of Engineering, University of Warwick, Coventry, UK*
T.Karavasilis@warwick.ac.uk

This paper evaluates the potential of SC-MRFs with viscous dampers to reduce the economic losses in steel buildings due to strong earthquakes. SC-MRFs are using the recently developed PT connection with web hourglass shape pins (WHPs) (Vasdravellis et al. 2013a; Vasdravellis et al. 2013b). The evaluation is based on the comparison of different designs of a prototype steel building using as lateral-load resisting system: 1) conventional steel moment resisting frames (MRFs); 2) MRFs with viscous dampers; 3) SC-MRFs; and 4) SC-MRFs with viscous dampers. The economic losses of these four design cases are estimated by developing vulnerability functions according to the ATC-58 (2012) methodology, which considers all repair costs associated with restoring the building to its original condition. The probability of demolition is also conditioned, by assuming different permissible residual storey drift levels.

SC-MRFs using PT connections and WHPs

Figure 1(a) shows a SC-MRF using PT connections with WHPs and Figure 1(b) show an exterior PT connection with WHPs. Figure 1(a) shows an exterior PT connection with WHPs. Two high strength steel bars located at the mid depth of the beam, one at each side of the beam web, pass through holes drilled on the column flanges. The bars are post-tensioned and anchored to the exterior columns. WHPs are inserted in aligned holes on the beam web and on supporting plates welded to the column flanges. Energy is dissipated through inelastic bending of the WHPs that have an optimized hourglass shape (Figure 1(c)) (Vasdravellis et al. 2013a; Vasdravellis et al. 2013b). The beam web and the beam flanges are reinforced with steel plates.

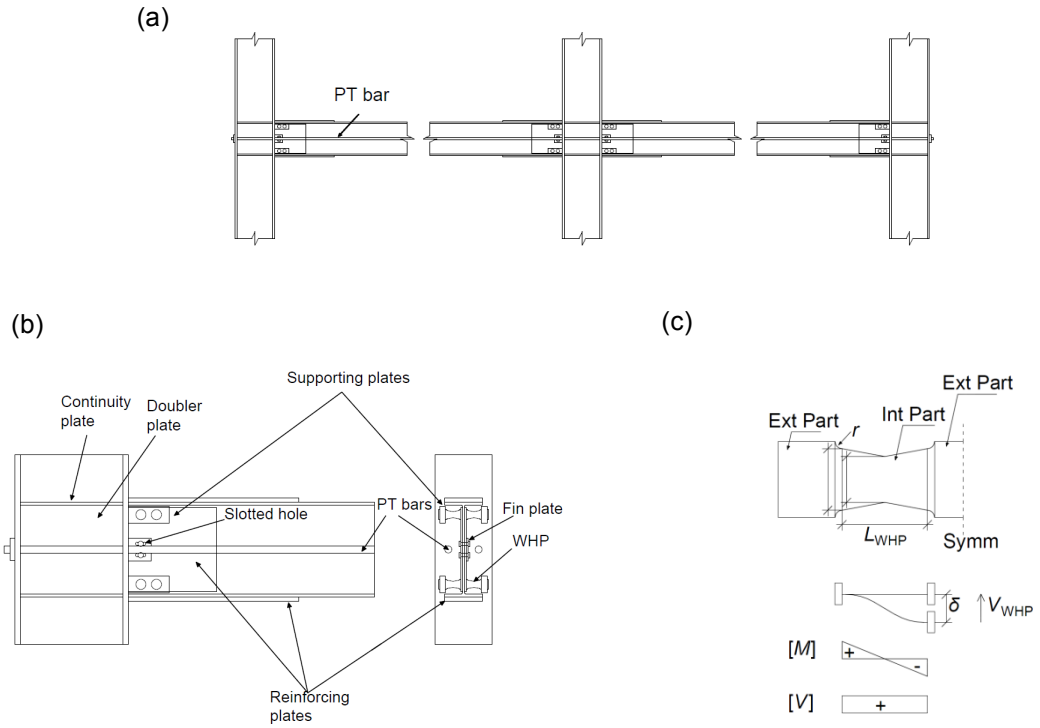

Figure 1. (a) SC-MRF; (b) exterior PT connection with WHPs; and (c) WHP geometry and assumed static system.

The connection behaviour is characterized by gap opening and closing in the beam-column interface as a result of the re-centering force in the PT bars. Figure 2(a) shows the free body diagram of an external PT connection where d_{1u} and d_{1l} are the distances of the upper and lower WHPs from the center of rotation that is assumed to be at the inner edge of the beam flange reinforcing plates; d_2 is the distance of the PT bars from the center of rotation; T is the total force in both PT bars; $F_{WHP,u}$ and $F_{WHP,l}$ are the forces in the upper and lower WHPs; C_F is the compressive force in the beam-column interface; V_{C1u} and V_{C1l} are the shear forces in

the upper and lower column, M is the PT connection moment, V is the beam shear force; and N is the horizontal clamping force that is transferred to the beam-column interface through the slab diaphragm and the beam. Figure 2(b) shows the SC-MRF expansion due to rotations θ in the PT connections.

Figure 2(c) shows the theoretical cyclic moment-rotation (M-θ) behaviour of the PT connection with WHPs, which has been verified by the large-scale experiments conducted by Vasdravellis et al. (2013a). After decompression of the PT connection (Point 1 in Figure 1(c)), gap opens and the behaviour becomes nonlinear elastic with rotational stiffness S_1. At point 2, the upper WHPs yield and M continues to increase with slope S_2. At point 3, the lower WHPs yield and M continues to increase with slope S_3. When loading is reversed, the connection begins to unload until the gap closes. More details about the connection behaviour can be found elsewhere (Vasdravellis et al. 2013a; Vasdravellis et al. 2013b; Tzimas et al. 2015).

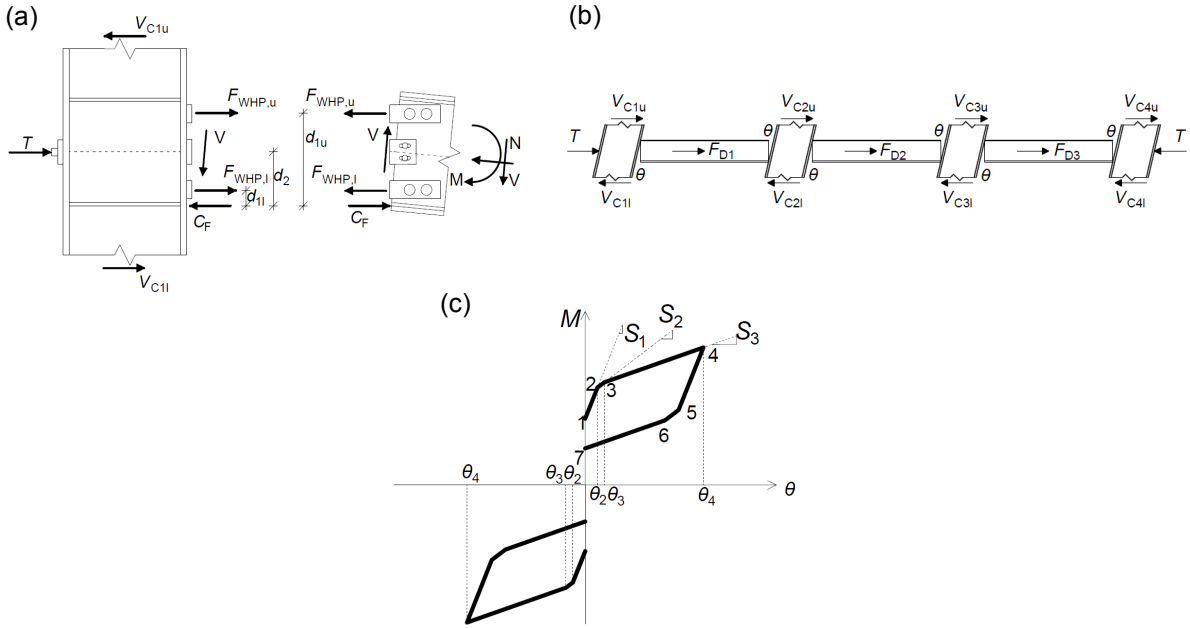

Figure 2. (a) Free body diagram of an external PT connection; and (b) SC-MRF expansion and horizontal forces equilibrium; (c) theoretical cyclic behaviour of the PT connections with WHPs.

Loss estimation procedure

The seismic loss of a building is split into three distinct types according to ATC-58: (a) structural losses, pertaining to damage in the load-carrying members of the structure, (b) non-structural loss for damage to non-load carrying components, such as partitions, piping systems, etc, and (c) contents loss. All three types are assessed using component fragility functions parameterized on the engineering demand parameters (EDP) (i.e. peak storey drift ($\theta_{s,max}$), peak floor accelerations (PFA)), which are recorded during the analysis. Following the ATC-58, at each intensity measure (IM) each component has a certain probability of being in any of its damage states (DS), which is in turn associated with a probabilistic cost function. Summing up such costs over the entire structure yields the total loss. Following the guidelines of ATC-58, the spectral acceleration at the fundamental period of vibration, $S_a(T_1)$, is chosen as IM.

The probability of collapse is explicitly incorporated as suggested by Aslani and Miranda (2005), i.e. collapse is assumed to cause instant loss of the entire building and its contents and can dominate vulnerability at higher IMs. The probability of demolition is also incorporated following Ramirez and Miranda (2012), i.e. by recognizing that the building will be demolished when a critical value of the residual storey drift ($\theta_{s,res}$) is exceeded. The

probability of having to demolish the structure conditioned on $\theta_{s,res}$, $P(D|\theta_{s,res})$, is assumed to follow a lognormal distribution with a logarithmic standard deviation of 0.3 according to Ramirez and Miranda (2012) and a median value that was assumed equal to 0.50% (McCormick 2008) and 1.88% (Jayaram et al. 2012) to allow a parametric study to be conducted.

Vulnerability functions are developed in this study using a simulation procedure based on the PEER (Pacific Earthquake Engineering Research) loss analysis framework (Cornell and Krawinkler 2000; Deierlein 2004). In the PEER framework, the mean annual frequency (MAF) of a Decision Variable (DV), such as the cost or the loss ratio (building loss to the building value), is estimated as

$$\lambda_{DV}(DV \geq dv) = \iiint G(dv|DS)\left|dG(DS|EDP)\right|\left|dG(EDP|IM)\right|\left|\frac{d\lambda(IM)}{dIM}\right|dIM \qquad (1)$$

Where $\lambda_{DV}(DV>dv)$ is MAF of exceeding 'dv' for the given site and building; $G(dv|DS)$ denotes the probability of exceedance of the dv given a DS (i.e., a damage state associated with a specific repair action, such as local beam flange and web buckling); $dG(DS|EDP)$ is the derivative of the probability of exceedance of the damage measure given an EDP; $dG(EDP|IM)$ is the derivative of the probability of exceedance of the EDP given an IM; $d\lambda(IM)$ is the derivative of the MAF of exceedance of an IM; and dIM is a differential element of infinitesimal length of IM. In this work the spectral acceleration at the structures fundamental period, denoted $S_a(T_1)$ is chosen as IM.

In this work, only a part of Equation (1) is used to assess the performance of a building in an objective manner that does not depend on the site, i.e. using only the integrals of $G(dv|DS)$ over EDP and DS without the final convolution with $\lambda(IM)$. The result is known as the vulnerability function:

$$G(DV|IM) = \iint G(dv|DS)\left|dG(DS|EDP)\right|\left|dG(EDP|IM)\right| \qquad (2)$$

Equation (2) computes DV as a function of IM and it is characteristic of the building and independent of the site. Monte Carlo Simulation (MCS) is used to evaluate the integrals shown in Equation (2). The MCS approach involves simulating all the random variables in Equation (2) (DV, EDP, DS, IM) and then computing the DV for a wide range of IM. The steps involved in the MCS approach are presented in detail by Jayaram et al. (2012).

Prototype building

Figure 3(a) shows the plan view of a 5-storey, 5-bay by 3-bay prototype building having two identical perimeter seismic-resistant frames in the 'x' plan direction. These frames are designed as conventional MRFs, MRFs with viscous damper, SC-MRFs and SC-MRFs with viscous dampers, based on existing design procedures (EC8 2008; Tzimas et al. 2015). All the buildings are designed to have the same cross sections. In such a way, buildings with different type of lateral-load resisting system will have the same fundamental period, but different structural performance under strong earthquakes. Viscous dampers are installed in the interior gravity frames as shown in Figure 3(b). For all the design cases, $\theta_{s,max}$ is less than 0.75% under the frequently occurred earthquake (FOE). The DBE is expressed by the Type 1 elastic response spectrum of EC8 with peak ground acceleration equal to 0.35g and ground type B. The FOE has intensity of 40% the intensity of the DBE. The maximum considered earthquake (MCE) has intensity of 150% the intensity of the DBE. The model used for the design is based on the centerline dimensions of the seismic-resistant frame without accounting for the finite panel zone dimensions. A 'lean-on' column is included in the model to account for the P-Δ effects of the vertical loads acting on the gravity columns in the tributary plan area (half of the total plan area) assigned to the seismic-resistant frame. A rigid diaphragm constraint is imposed at the nodes of each floor level for the design. The steel

yield strength is equal to 355 MPa for the columns, 275 MPa for beams, 930 MPa for PT bars, 235 MPa for the WHPs and 275 MPa for the beam reinforcing plates. Nonlinear viscous dampers are designed with a horizontal configuration (as shown in Figure 3(b)) and a velocity exponent equal to 0.5 to achieve a total damping ratio equal to 20% at the first fundamental period, which is equal to T_1=1.27 s. The estimated $\theta_{s,max}$ under the DBE is equal to 1.20% and 1.80% for the MRFs and SC-MRFs with and without dampers, respectively. Design data of the frames are given in Table 1.

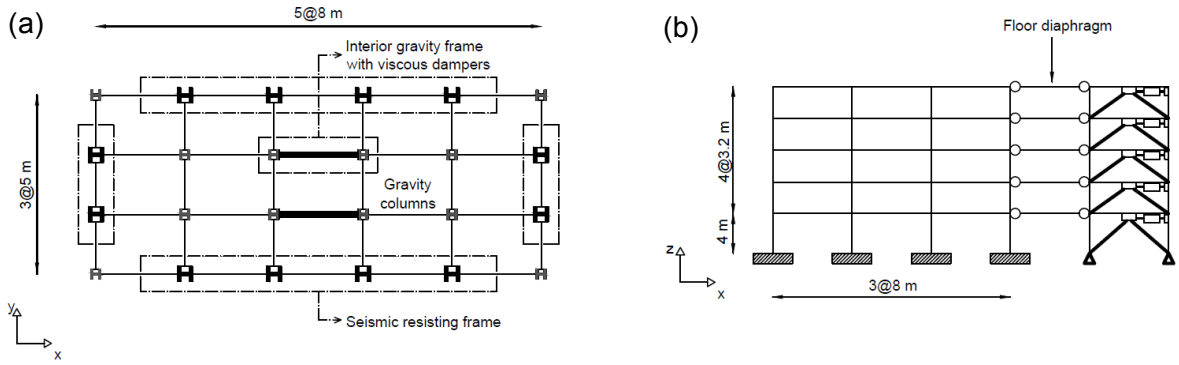

Figure 3. (a) Plan view of the prototype building; (b) Elevation view of the prototype building

Table 1. Design data of the steel MRF, SC-MRF and viscous dampers

	Cross sectios		PT force	PT bar diameter	WHPs with L_{whp} = 70mm		Reinf. plate length	Reinf. plate thickness	Viscous dampers
Storey	Beam	Column	T_0 (kN)	d_{PT} (mm)	D_e (mm)	D_i (mm)	L_{rp} (mm)	t_{rp} (mm)	c (kN·(s./m)$^{0.5}$)
1	IPE550	HEB650	1087	50	43	33	1392	35	2139
2	IPE600	HEB650	1256	60	46	36	1660	46	1641
3	IPE550	HEB650	1087	48	43	33	1416	35	1416
4	IPE500	HEB600	941	38	41	30	1092	26	1102
5	IPE500	HEB600	941	36	39	28	743	22	810

To evaluate the performance of the prototype building of Figure 3 in terms of repair and replacement cost, it is assumed that the building includes the structural components, non-structural components and contents listed in Table 2. Table 2 lists the component, the associated ATC-58 identification (ID), the component units that the building includes per storey, and the associated EDP used to assess the component DS.

The fragility and cost functions of the PT connections are not provided by ATC-58. On the basis of limited information, market research and engineering judgement are used to determine these functions. It is assumed that DSs in the PT connections are associated with the replacement of WHPs under the DBE and the plastic hinge rotation, θ_p, at the end of the reinforcing beam flange plate. θ_p is associated to $\theta_{s,max}$ on the basis of pushover analysis. PT bar yielding is not considered as a DS, because it is not critical failure mode in the current design cases (Dimopoulos et al. 2015). For the definition of fragility functions, equations presented in Chapter 3 of ATC-58 are used. The cost functions related to WHPs and θ_p at the end of the reinforcing beam flange plate were determined based on the mean and dispersion values of the corresponding conventional moment resisting connections. The contents cost functions have been developed based on USA market prices.

Models for non-linear analyses

A simplified nonlinear model for PT connections with WHPs has been developed in OpenSees. In this model the PT connections and the associated beams and columns, consist of nonlinear beam-column elements and hysteretic spring elements, appropriately placed in the beam-column interface. The strength and stiffness deterioration of the beams due to plastic hinge rotation were also taken into consideration. The connections of the

conventional MRFs are assumed to be rigid and have full strength, while the effect of strength and stiffness deterioration of the beams due to plastic hinge rotation were also taken into consideration. P-Δ effects are taken into consideration. A detailed description of the models of this study can be found in the work of Dimopoulos et al. (2015). The OpenSees models for the SC-MRFs and the conventional MRFs include the effect of the panel zone stiffness, and so, result in T_1 value shorter than 1.27 s that is based on the centerline models used for design. T_1 from the OpenSees models is 0.94 s for both SC-MRFs with and without viscous dampers and 1.18 s for both MRFs with and without viscous dampers.

Table 2. Prototype building components per storey

MRF components	ATC-58 (ID)	SC-MRF components	units	EDP
Steel column base plate	B1031.011b	-//-	8	$\theta_{s,max}$
Post-Northridge welded steel moment connection, beam one side	B1035.021 / None	PT connection, beam one side	4	$\theta_{s,max}$
Post-Northridge welded steel moment connection, beams both sides	B1035.031 / None	PT connection, beams both sides	4	$\theta_{s,max}$
Bolted shear tab gravity connections	B1031.001	-//-	28	$\theta_{s,max}$
curtain walls	B2022.001	-//-	54	$\theta_{s,max}$
suspended ceiling	C3032.003a	-//-	26	PFA
cold water piping	D2021.011a	-//-	1	PFA
hot water piping	D2022.012b	-//-	1	PFA
HVAC	D3041.001a	-//-	3	PFA
Modular office work stations	E2022.001	-//-	90	PFA
unsecured fragile objects on shelves	E2022.010	-//-	90	PFA
electronic equipment on wall	E2022.021	-//-	1	PFA
Desktop electronics	E2022.022	-//-	90	PFA
Book case	E2022.102a	-//-	90	PFA

Nonlinear dynamic analyses and collapse simulation

To investigate sidesway collapse, incremental dynamic analysis (IDA) (Vamvatsikos and Cornel 2002) is performed for all the deign cases (SC-MRF, SC-MRF with viscous dampers, MRF and MRF with viscous dampers). IDA involves increased amplitude scaling of individual ground motion records to estimate the relationship between IM and EDP. For the IDA simulations, sidesway collapse is defined as the point of dynamic instability when $\theta_{s,max}$ increases without bound. IDAs were performed under a set of 22 recorded far-field ground motions pairs (i.e. 44 time histories) developed by the ATC-63 project. The Newmark method with constant acceleration is used to integrate the equation of motions. A Rayleigh damping matrix is used to model the inherent 3% critical damping at the first two modes of vibration. Each dynamic analysis is extended well beyond the actual earthquake time to allow for damped free vibration decay and accurate $\theta_{s,res}$ calculation.

Figure 4 shows the collapse fragility curves of all the design cases, where the $S_a(T_1)$ is normalized by $S_{a,MCE}$, i.e. the MCE spectral acceleration of the ground motion at T_1. All the examined design cases, shown in Figure 4, have superior collapse resistance, with zero probability of collapse under the MCE. SC-MRF has significantly better performance with fragility curves clearly shifted to the right of the MRF. The use of viscous dampers results in higher collapse resistance for both the MRF and the SC-MRF, with the corresponding collapse fragility curves shifted to the right.

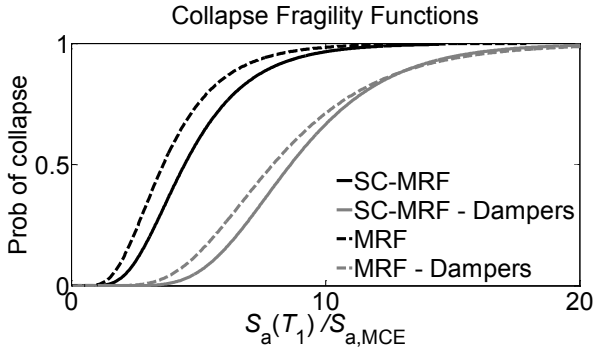

Figure 4. Collapse fragility function of all design cases, normalized to $S_{a,MCE}$

Estimation of economic seismic losses

Figure 5 shows the vulnerability functions of all the design cases at 50% probability of exceedance of a DV for a wide range of IMs, by assuming that the median and lognormal standard deviation of $P(D|\theta_{s,res})$ are equal to 1.88% and 0.30, respectively. The selected DVs are the repair cost and the loss ratio.

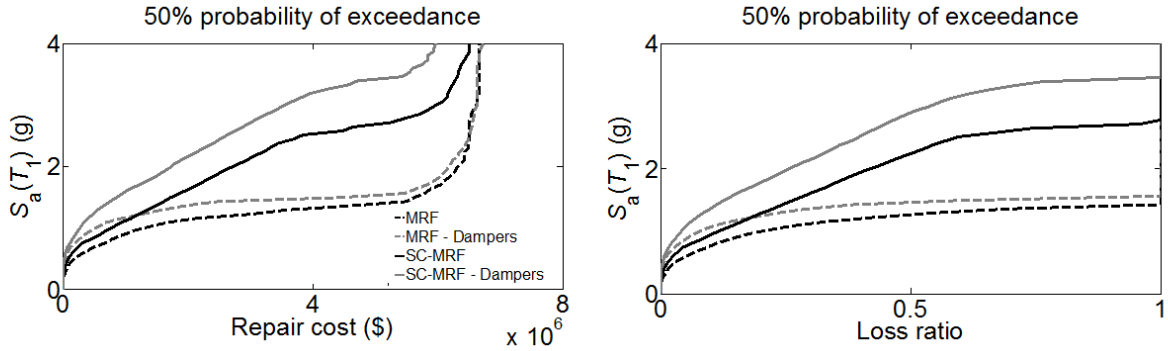

Figure 5. 50% probability of a DV to be exceeded, expressed in terms of repair cost and loss ratio, for a wide range of IMs and median of $P(D|\theta_{s,res})$ equal to 1.88%

The SC-MRFs with and without viscous dampers have better performance compared to the corresponding MRFs, with their vulnerability function shifted to the top of Figure 5. Also, both MRF and SC-MRF have better performance when viscous dampers are inserted into the building. The SC-MRF with viscous dampers has higher performance with vulnerability functions clearly shifted to the top of those of the other frames. This demonstrates the effectiveness of supplemental damping to improve the structural and non-structural seismic performance of steel SC-MRFs by minimize $\theta_{s,res}$ under high seismic intensities. The 50% probability of repair cost to be exceeded for each design case is presented in Table 3, under several seismic intensities.

The results in Table 3 show that viscous dampers reduce by more than 90% the repair cost for both MRF and SC-MRF under the MCE and DBE, while they minimize it under the FOE. SC-MRFs with and without viscous dampers have similar performance with the corresponding MRFs, under the FOE, DBE and MCE. For $S_a(T_1)$=1.0g the repair cost of both MRF and SC-MRF is reduced by more than 50% when viscous dampers are inserted into the building; SC-MRFs with and without viscous dampers reduce the repair cost by 50% and 40% compared to the corresponding MRFs, respectively. For $S_a(T_1)$=2.0g and $S_a(T_1)$=3.0g, viscous dampers are more effective into the SC-MRF. For $S_a(T_1)$=2.0g the SC-MRFs with and without viscous dampers reduce the repair cost by 72% and 56% compared to the corresponding MRFs, respectively. For $S_a(T_1)$=3.0g the SC-MRF with viscous dampers has significantly better performance than the other design cases (45% reduction in repair cost). The aforementioned results demonstrate the crucial role of $\theta_{s,res}$ by considering the losses

resulting from the $P(D|\theta_{s,res})$ and the ability of the SC-MRFs to reduce the repair cost by minimize $\theta_{s,res}$, under high seismic intensities.

Table 3. 50% probability of repair cost to be exceeded in \$ (10^6). Buildings with median of $P(D|\theta_{s,res})$ equal to 1.88%

Design cases	$S_{a,FOE}$	$S_{a,DBE}$	$S_{a,MCE}$	$S_a(T_1)$=1.0g	$S_a(T_1)$=2.0g	$S_a(T_1)$=3.0g
MRF	0.01	0.15	0.50	1.39	6.37	6.64
MRF - Dampers	0.00	0.01	0.02	0.57	6.20	6.63
SC-MRF	0.01	0.13	0.45	0.82	2.80	6.07
SC-MRF - Dampers	0.00	0.01	0.04	0.29	1.78	3.67

Figure 6 shows the vulnerability functions of all the design cases at 50% probability of exceedance of a DV for a wide range of IMs, by assuming that the median and lognormal standard deviation of $P(D|\theta_{s,res})$ are equal to 0.5% and 0.30, respectively. The selected DVs are the repair cost and the loss ratio.

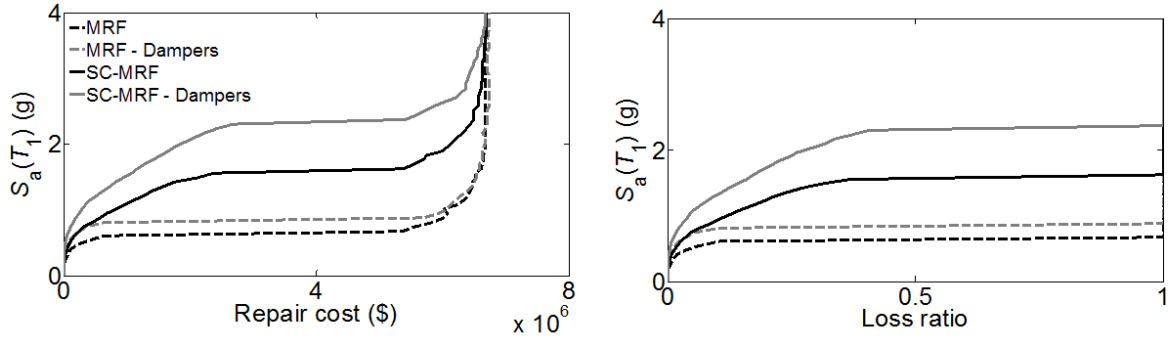

Figure 6. 50% probability of a DV to be exceeded, expressed in terms of repair cost and loss ratio, for a wide range of IMs and median of $P(D|\theta_{s,res})$ equal to 0.5%

The results in Table 4 show that viscous dampers minimize the repair cost for both MRF and SC-MRF under the FOE, DBE and MCE. The SC-MRFs with and without viscous dampers have similar performance with the corresponding MRFs, under the FOE and DBE. Under the MCE, the SC-MRF has a significantly reduced repair cost (90%) than the MRF, while the SC-MRF with viscous dampers has similar performance with the MRF with viscous dampers. For $S_a(T_1)$=1.0g and $S_a(T_1)$=2.0g viscous dampers are more effective only into the SC-MRF, where they result in 69% reduction of repair cost, while the repair cost of the MRF does not significantly changes when viscous dampers are inserted. In addition, for $S_a(T_1)$=1.0g the SC-MRFs with and without viscous dampers reduce the repair cost by 95% against the corresponding MRFs with and without viscous dampers. For $S_a(T_1)$=3.0g viscous dampers are not effective for both MRF and SC-MRF, while the SC-MRF with and without viscous dampers has similar performance with the MRFs with and without viscous dampers respectively.

Table 4. 50% probability of repair cost to be exceeded in \$ (10^6). Buildings with median of $P(D|\theta_{s,res})$ equal to 0.5%

Design cases	$S_{a,FOE}$	$S_{a,DBE}$	$S_{a,MCE}$	$S_a(T_1)$=1.0g	$S_a(T_1)$=2.0g	$S_a(T_1)$=3.0g
MRF	0.01	0.14	5.36	6.02	6.67	6.68
MRF - Dampers	0.00	0.01	0.03	6.06	6.67	6.73
SC-MRF	0.01	0.13	0.45	0.83	6.15	6.63
SC-MRF - Dampers	0.00	0.01	0.04	0.29	1.92	6.41

Comparison between the results of Table 3 and 4 shows that by using median of $P(D|\theta_{s,res})$ equal to 0.5%, the SC-MRF has 90% reduced repair cost compared to the MRF repair cost

under the MCE, while by using median of $P(D|\theta_{s,res})$ equal to 1.88% both MRF and SC-MRF under the MCE and DBE have similar repair cost. The aforementioned results demonstrate the crucial role of $\theta_{s,res}$ by considering the losses resulting from the $P(D|\theta_{s,res})$, since it can affect the selected type of lateral resisting system. Nevertheless, more work is needed to evaluate the $\theta_{s,res}$ beyond which the structure can be demolished.

Conclusion

In this paper the potential of SC-MRFs with viscous dampers to reduce the economic losses in steel buildings due to strong earthquakes is evaluated. The evaluation is based on the comparison of different designs of a prototype steel building using as lateral-load resisting system: 1) conventional steel MRFs; 2) MRFs and viscous dampers; 3) SC-MRFs; and 4) SC-MRFs with viscous dampers. The building's repair cost is evaluated by developing vulnerability functions according to the state of the art ATC-58 methodology, and compared for all the design cases. The probability of demolition after a strong earthquake was also taken into account by assuming different permissible residual storey drifts levels. Based on the results presented in the paper, the following conclusions are drawn:

1. All the design cases have zero probability of collapse under the MCE. The SC-MRF has higher collapse resistance compared to the corresponding MRF. The use of viscous dampers results in higher collapse resistance for both the MRF and the SC-MRF, while the SC-MRF with viscous dampers has superior collapse resistance.
2. The use of viscous dampers reduces the repair cost by more than 90% for both the MRF and SC-MRF under the MCE and DBE, while the repair cost is minimized under the FOE.
3. SC-MRFs with and without viscous dampers have similar performance to that of the corresponding MRFs, up to the MCE. For higher seismic intensities (e.g. $S_a(T_1)$=2.0g), SC-MRFs with and without viscous dampers have significantly improved performance compared to the corresponding MRFs and lower repair cost, while the effect of dampers is considerable in the case of the SC-MRF.
4. The results show that if the probability of having to demolish the structure conditioned the residual storey, $P(D|\theta_{s,res})$, has low median value then the SC-MRFs with or without viscous dampers have better performance compared to the corresponding MRFs. However, for high median values of $P(D|\theta_{s,res})$ and seismic intensities up to MCE both MRF and SC-MRF have similar economic losses.
5. The results highlight the importance of considering residual drifts as a demand parameter controlling whether a building is repairable or needs to be demolished in the aftermath of a strong earthquake.

Acknowledgements

Financial support for this work is provided by the Engineering and Physical Sciences Research Council of the United Kingdom; Grant Ref: EP/K006118/1.

REFERENCES

Applied Technology Council (ATC) (2012) *ATC-58: Guidelines for Seismic Performance Assessment of Buildings*, 100% Draft. Redwood City, CA

Aslani H, Miranda E. (2005) *Probabilistic earthquake loss estimation and loss disaggregation in buildings*, *Report No. 157*, The John A. Blume Earthquake Engineering Research Center, Stanford University, Stanford, CA

Deierlein GG (2004) *Overview of a comprehensive framework for earthquake performance assessment*, Technical report, International Workshop on Performance-Based Seismic Design Concepts and Implementation, Bled, Slovenia

Dimopoulos AI, Tzimas AS, Vamvatsikos D and Karavasilis TL (2015) Economic seismic losses in steel buildings using self-centering post-tensioned moment-resisting frames and viscous dampers, *Earthquake Engineering and Structural Dynamics*, Under review

Cornell CA and Krawinkler H (2000) Progress and challenges in seismic performance assessment, *PEER Center News*, 3(2):1–4

EC8 - Eurocode 8 (2008) *Design of structures for earthquake resistance*

FEMA P695 (2008) *Quantification of building seismic performance factors*, ATC-63 Project, Applied Technology Council, CA, USA

Garlock M, Sause R and Ricles JM (2007) Behavior and design of posttensioned steel frame systems, *Journal of Structural Engineering*, 133(3): 389-399

Jayaram N, Shome N and Rahnama M (2012) Development of earthquake vulnerability functions for tall buildings, *Earthquake Engineering and Structural Dynamics*, 41:1495-1514

Kim H and Christopoulos C (2008) Seismic design procedure and seismic response of post-tensioned self-centering steel frames, *Earthquake Engineering and Structural Dynamics*, 38(3): 355-376

McCormick J, Aburano H, Ikenaga M, Nakashima M (2008) *Permissible residual deformation levels for building structures considering both safety and human elements*, Proc. 14th world conference in Earthquake Engineering, Seismological Press of China, Paper ID 05-06-0071, Beijing

OpenSees (2013), *Open system for earthquake engineering simulation*, Pacific Earthquake Engineering Research Center, University of California at Berkeley, Berkeley, CA

Ramirez CM and Miranda E (2012) Significance of residual drifts in building earthquake loss estimation, *Earthquake Engineering and Structural Dynamics*, 41:1477-1493.

Tzimas AS, Dimopoulos AI and Karavasilis TL (2015) EC8-based seismic design and assessment of self-centering post-tensioned steel frames with viscous dampers, *Journal of Constructional Steel Research*, 105: 60-73

Vamvatsikos D and Cornell CA (2012) Incremental dynamic analysis, *Earthquake Engineering and Structural Dynamics*, 31(3): 491-514

Vasdravellis G, Karavasilis TL and Uy B (2013a) Large-scale experimental validation of steel post-tensioned connections with web hourglass pins, *Journal of Structural Engineering*, 139(6): 1033-1042

Vasdravellis G, Karavasilis TL and Uy B (2013b) Finite element models and cyclic behaviour of self-centering post-tensioned connections with web hourglass pins, *Engineering Structures*, 52:1-16